2016

Lentiviral GFP Transfection of the Parthenogenic Crayfish Species, Procambarus fallax: A Tool for Examining the Source of Neural Precursor Cells In Crayfish

Zena Chatila
zchatila@wellesley.edu

Lentiviral GFP Transfection of the Parthenogenic Crayfish Species, *Procambarus fallax*: A Tool for Examining the Source of Neural Precursor Cells In Crayfish

Zena Chatila
Advisor: Barbara Beltz
Neuroscience Program

Submitted in Partial Fulfillment of the
Prerequisite for Honors in Neuroscience

April 2016

Acknowledgements

I would like to recognize and thank all of those who helped me and provided me with guidance and support, and without whom this thesis would not have been possible.

My advisor, professor Barbara Betlz, whom I thank deeply for her mentorship and guidance over the course of my time working in her lab and with my thesis project. She has taught me more than I can express and has made my academic experience at Wellesley unforgettable. She has imparted unto me her wonderful enthusiasm and excitement for research, which I will carry forward for the rest of my career.

Jeannie Benton, whom I thank for her immense help and advice on my project, for training me at the bench, and for her constant support. She creates such a wonderfully encouraging environment in the lab, and I cannot imagine my research experience without her.

Georg Brenneis, whom I thank for his advice, for his guidance as my project became more difficult, and for his sarcasm.

Virginia Quinan, whom I thank for generously spending hours teaching me western blots, for her role on my thesis committee, and for her constant enthusiasm and support for my project.

Marc Tetel, whom I thank for serving on my thesis committee despite being on sabbatical, and for his thoughtful advice on my project.

Kara Banson, Megan McNeil, and Anushree Dugar, whom I thank for being such wonderful lab members and making my experience in the Beltz lab such an enjoyable one.

To Pat Carey and Val LePage from the Wellesley Animal Care Facility whom I thank for looking after our animals, and for helping me as I constantly shifted animals around during my experiments.

The Arnold and Mabel Beckman Foundation, which I thank for funding for my research.

My wonderful friends at Wellesley, specifically Leila Elabbady, Broti Gupta, and Mariya Patwa, whom I thank for letting me endlessly complain to them, for their wise advice, and for their constant care, encouragement, and support.

Majed Alnahwi, whom I thank for feeding me after long days in the lab, for instilling confidence in me, for listening to me constantly talk about my research without losing interest, and for his love and support.

My family whom I thank for their encouragement, for their excitement for my research, and for their constant love.

Koosah, my cat, whom I thank for being a wonderful writing companion and for keeping me company during long hours of editing.

Table of Contents

Index of Figures

Abstract

In crayfish, neuronal stem cells (NSCs) are not self-renewing, yet adult neurogenesis continues throughout an animal's life without depleting the small stem cell population in the neurogenic niche. Thus, NSCs in crayfish must be replenished from a source external to the niche. Experiments have demonstrated that hemocytes (blood cells) generated by the immune system are competent to become neuronal precursor cells, and are a likely source of the NSCs involved in adult neurogenesis in crayfish. While the brain cells derived from these hemocyte precursors express neurotransmitters, it is not known whether they are fully functional and form neural connections. The aim of the present work, therefore, was to develop methods by which newborn neurons can be identified and located for *in vivo* electrophysiological analysis. The first goal was to establish a method for creating transgenic crayfish (*Procambarus fallax*) expressing green fluorescent protein (GFP) in the hematopoietic tissues that generate blood cells, by exposing animals to a lentiviral vector at key points in early post-embryonic development. GFP expression in tissues of the immune system and in hemocytes was confirmed with confocal microscopy. Additional studies are testing approaches for increasing GFP expression. In future experiments, GFP+ animals will act as hemocyte donors, providing labeled blood cells to recipients that can be visualized in living tissues, as GFP will be expressed in donor cells and their descendants. The ultimate goal is to conduct electrophysiological studies on cells derived from GFP+ donors in the recipient crayfish, to determine whether these cells create functional synapses and gain the electrical properties necessary to act as fully functioning neurons. Our hypothesis is that brain cells derived from GFP+ hemocytes will differentiate into fully functional neurons. Further, the standard crayfish brain preparation developed for electrophysiology accesses brain regions and perfuses blood vessels from the dorsal surface.

Therefore, in order to determine an appropriate electrophysiological approach for these experiments, a second goal of these studies was to quantitatively assess newborn cell movement throughout the brain, from the ventral region where they are initially integrated, to more dorsal regions. Seven to eight weeks after the arrival of cells in cluster 10 from the migratory streams, a stable, sizable population of newborn cells was found to reside in the dorsal third of the brain, suggesting that after this time a dorsal electrophysiological approach may be used. These studies therefore address two critical issues related to electrophysiological studies of the newborn neurons: (1) generating transgenic crayfish that produce GFP+ blood cells for use in adoptive transfers, and (2) tracking the movement of cells within the brain to determine when these are accessible using current electrophysiological approaches.

Introduction

Adult Neurogenesis

For decades, it was commonly believed that new brain cells, or neurons, could not be produced in humans after development, and that the adult brain contained a static pool of neurons that slowly degenerate with age. However, in 1998, a remarkable study demonstrated that this process, known as adult neurogenesis, does occur in the human brain (Eriksson et al., 1998). This phenomenon has been demonstrated in all vertebrate species that have been examined, as well as in the majority of non-vertebrates (Kempermann, 2000; Sullivan et al., 2007). Adult neurogenesis has now become widely accepted as a common occurrence. In the mammalian brain, neurogenesis occurs in the subventricular zone, which contributes new neurons to the olfactory bulb, and the subgranular zone in the hippocampus (Altman and Das, 1965; Cameron et al., 1993; Rousselot et al., 1995; Doetsch et al., 1997; Garcia-Verdugo et al., 2002; Zhao et al., 2008). While these two brain regions experience the highest levels of adult

neurogenesis, this process is also thought to occur in other brain areas including the hypothalamus and the striatum, although less is known about these pathways (Bédard et al., 2002; Kokoeva et al., 2007).

Adult neurogenesis is believed to underlie mechanisms of neural plasticity, learning and memory (Parent et al., 1997; van Praag et al., 1999; Magavi et al., 2000). In addition, this phenomenon may be critical for regeneration of damaged neural tissue (Liu et al., 1998). Dysfunctions in adult neurogenesis have been implicated in several psychiatric and neurodegenerative diseases, including clinical depression and epilepsy (Jacobs et al., 2000; Pun et al., 2012). Furthermore, neural stem cells, from which adult-born neurons are derived, appear to be the basis for many primary brain tumors (Uchida et al., 2000; Dirks, 2010; Germano et al., 2010). Thus, an understanding of adult neurogenesis is of critical importance, and may lead to new medical treatments targeting these diseases.

Invertebrate Models in Neuroscience

The field of neuroscience has made great use of invertebrate systems and the advantages they present over more complex mammalian systems. Several studies in invertebrate models have elucidated basic neural mechanisms. For example, ionic flow of current across the axonal membrane was determined in squid giant axon (Hodgkin and Huxley, 1952), and the synaptic basis of learning and memory was discovered in *Aplysia californica* (Cedar et al., 1972). As neural mechanisms are widely conserved across species, these findings have informed us as to some of our most basic neural processes and have since been demonstrated in mammalian systems including humans (Bear et al., 2007; Kokovay et al., 2008).

Mechanisms of adult neurogenesis appear to be highly conserved evolutionarily, as there are many similarities in fundamental mechanisms across a broad range of species. In all species

examined, neural stem cells (NSCs, self-renewing undifferentiated cells with the potential to produce neurons and glia) residing in a highly vascularized niche produce a lineage of three to four generations of cells (Steiner et al., 2006; Sullivan et al., 2007; Zhao et al., 2008). The final generation of this lineage then differentiates into neurons. Precursor cells must migrate from the niche to the site of differentiation, where they ultimately integrate into neural circuits. In the Beltz lab, crustaceans (e.g., lobsters, crayfish) have been used to study mechanisms of adult neurogenesis as they undergo lifelong neurogenesis and offer advantages over more traditional models such as rodents (Schmidt and Demuth, 1998; Beltz et al., 2011; Benton et al., 2014). Specifically, crayfish (and other invertebrates) have orders of magnitude fewer neurons compared to mammals. A small neural population is experimentally advantageous as fewer cells are more readily quantifiable, and therefore any manipulations or changes that occur in the system are more easily observed. Additionally, as crayfish undergo lifelong neurogenesis and have a defined lineage of neuronal precursor cells with generations that are spatially separated in the brain, the stage in the neuronal lineage can be determined by cell location (Zhang et al., 2009). Crayfish are therefore an ideal model for examining mechanisms of adult neurogenesis. As processes generating adult-born neurons are conserved across a diverse range of species (Kempermann et al., 1997; Nilsson et al., 1999; Sandeman and Sandeman, 2000; Ayub et al., 2011; Beltz et al., 2011), it is expected that findings in crayfish will have implications for our understanding of adult neurogenesis in evolutionarily more advanced species, including humans.

Neurogenesis in the Crayfish Brain

While the anatomical organization of the crayfish brain (Fig. 1A) differs greatly from the mammalian brain, at the cellular level neurons are very similar, for example in terms of chemistry and biophysics. Like the mammalian brain, the crayfish brain is positioned behind and

between the eyes and is bilaterally symmetrical. The crayfish brain contains two prominent neural regions, the olfactory lobe, which is analogous to the mammalian olfactory bulb, and the accessory lobe, a higher processing area that is most closely analogous to the mammalian hippocampus. In crayfish, the first generation neural precursor cells (NPCs), which are functionally analogous to neural stem cells in mammals, reside in the neurogenic niche, a highly vascularized structure that rests on the ventral surface of the accessory lobe, just beneath the brain sheath (Schmidt, 2007). However, unlike NSCs that undergo asymmetrical divisions, first generation NPCs undergo mitosis to produce two geometrically symmetrical daughter cells. These second generation NPCs then travel out of the niche and along tracts (known as migratory streams, created by the fibers of bipolar niche cells), towards the medial proliferation zone (MPZ, cluster 9) and the lateral proliferation zone (LPZ, cluster 10) (Fig. 1; Zhang et al., 2009; Benton et al., 2011). Once in the proliferation zones, the second generation NPCs undergo at least one more division producing third and

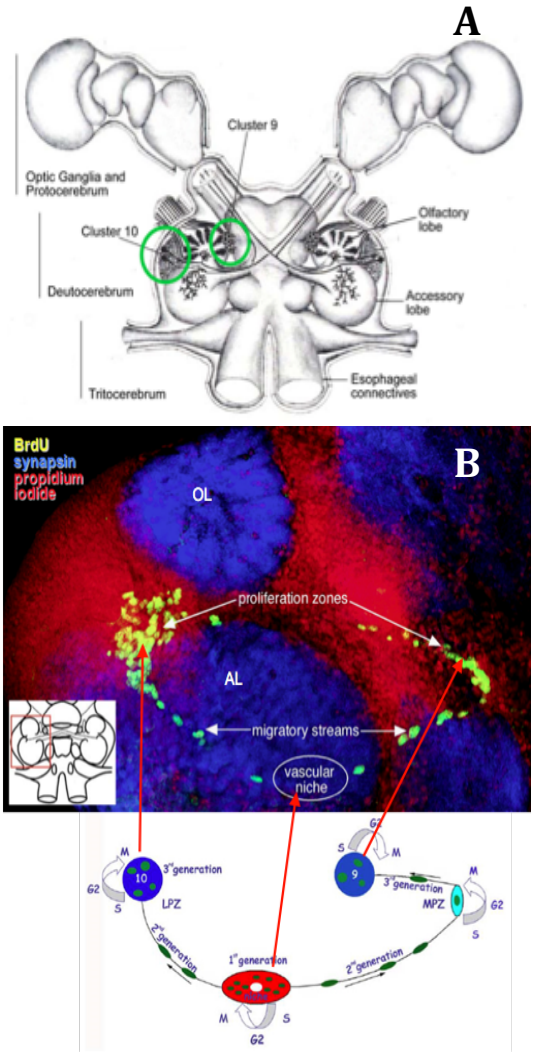

Figure 1. *The crayfish brain and pathway of neurogenesis.* (A) Schematic of crayfish brain, clusters 9 and 10 are indicated with green circles (Beltz et al., 2011). (B) Schematic of events leading to production of new neurons, matched with a corresponding image of the pathway, Green – BrdU, Red – Propidium Iodide, Blue – Synapsin (Sullivan et al., 2007).

subsequent generation cells, before progeny differentiate into neurons (Sandeman et al., 1992; Sullivan et al., 2007). New neurons integrate into brain cell clusters 9 and 10, and project to the olfactory and accessory lobes (Sandeman et al., 1992; Sullivan and Beltz, 2005).

Tools for Examining Adult Neurogenesis

Neurons do not divide, and are dependent on stem cells to maintain their population. Neural precursors undergo a series of divisions before their progeny differentiate into neurons. Therefore, it is possible to label newborn neurons with mitotic markers. Bromodeuoxyuridine (BrdU) and 5-ethnyl-2'-deoxyuridine (EdU) are both thymidine analogues and act as nucleoside labels, as they incorporate into cells during the S phase of the cell cycle. Cells containing either BrdU or EdU can be visualized with confocal microscopy, after tissues treated with either marker have been processed immunohistochemically (BrdU) or chemically (EdU). In crayfish, as the clearing time of BrdU and EdU is 48 hours (Benton et al., 2011), both of these markers label cells that have gone through S phase within 48 hours of injection. As a result, one can determine how many NPCs have divided within a 48-hour time period and can examine the rate at which neurogenesis occurs. The ability to label and subsequently quantify newborn neurons creates the opportunity to experimentally examine how rates of neurogenesis change when manipulations are introduced into the system, and to track cells within the neural precursor lineage as they progress towards differentiation.

Mind the Gap

In vertebrates, neural stem cells are thought to be self renewing (Zhao et al., 2008), meaning that they divide asymmetrically so that one daughter cell remains an undifferentiated stem cell and the other gives rise to a differentiating (neuron-producing) lineage. One piece of

the stem cell hypothesis is the long-term self-renewal of NSCs, such that a lifetime supply of NSCs is stored in the brain from birth (NIH, http://stemcells.nih.gov/info/basics/pages/basics2.aspx). However, while long-term self-renewing divisions are a hallmark of NSCs *in vitro* (Suh et al., 2007), there is no evidence that long-term self-renewal occurs *in vivo*. In fact, recent studies have shown very limited self-renewal among NSCs in both the subgranular and subventricular zones (Encinas et al., 2011; Calzolari et al., 2015; Fuentealba et al., 2015). In crayfish, neural precursor cells are not self-renewing, as first generation NPCs undergo divisions in which both daughter cells migrate away from the niche and give rise to subsequent differentiating generations (Zhang et al., 2009; Benton et al., 2011; Benton et al., 2013). Neural precursor cells were demonstrated to be non self-renewing by Benton et al. (2013) with a double nucleoside labeling experiment in which freshwater crayfish *Procambarus clarkii* were treated with BrdU and then EdU 3.5-7 days later. First generation NPCs in the niche did not retain a BrdU label as they would have if they underwent asymmetrical divisions in which one cell migrated away and the other cell remained in the niche. Instead, first generation NPCs were only labeled with the second nucleoside, EdU, and BrdU labeling was found selectively in the second generation NPCs along the migratory streams and in later generations in brain cell clusters where differentiation occurs. These results demonstrate that first-generation NPCs do not self-renew. Despite this fact, the neural precursor cell population in the neurogenic niche (which is approximately 300 cells in large adult crayfish [Zhang et al., 2009]), is not depleted, and adult neurogenesis continues throughout the animal's long life, which can span from fifteen to twenty years. Importantly, NPCs undergo one division every 48 hours, indicating that 300 NPSs are inadequate to sustain lifelong adult neurogenesis in

crayfish (Benton et al., 2011). Thus, NPCs must be replenished from a source external to the niche (Zhang et al., 2009; Benton et al., 2013).

The existence of an external source of NPCs was demonstrated by the Beltz lab through studies in which animals were injected with BrdU and the presence of labeled cells in the niche was examined at various time points up to 21 days after injection (Fig. 2; Benton et al. 2014). First generation precursor cells residing in the niche were labeled with BrdU on days 1-4 after injection. No labeled cells were observed in the niche from days 5-7 after injection. This result was expected, as the cell cycle time for niche precursor cells is 48 hours at minimum (Benton et al., 2011). Therefore, 5-7 days post injection falls after the 48 hour clearing time of BrdU and the additional 48 hours required for any BrdU-labeled first generation precursors to complete the cell cycle and migrate from the niche (Benton et al., 2011). However, on days 8-14 after injection, BrdU-labeled cells were again observed in the niche, long past the BrdU clearing time. As BrdU is no longer readily available to label cells residing in the niche, these labeled cells must have incorporated BrdU in their source tissues at the time of the initial injection and then migrated to the niche. It has been concluded that the time between BrdU injection and the arrival of labeled

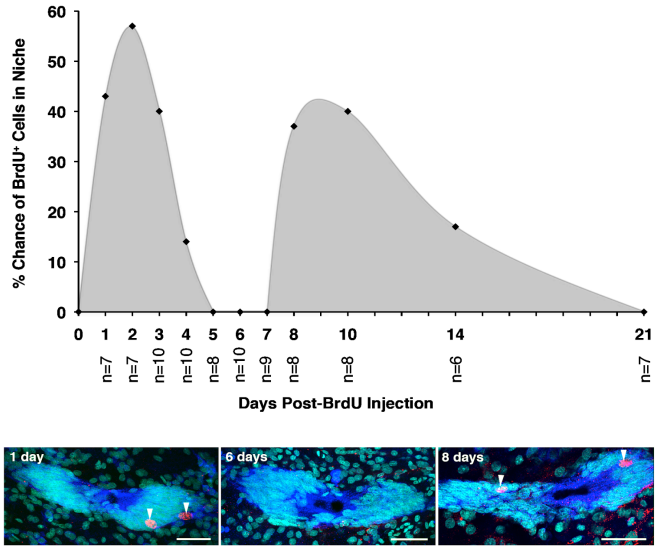

Figure 2. *BrdU cells appear in the niche after a "gap" period, days after the BrdU clearing time.* BrdU-labeled cells were quantified in the niches of crayfish that were sacrificed at varying intervals after BrdU injection. The likelihood of BrdU-labeled cells residing in the niche was plotted over time, for each of the sampling days post injection. BrdU-labeled cells were observed in the niche between days 1-4, none were observed from days 5-7, and between days 8-14, BrdU-labeled cells were again observed in the niche. Images of niches on days 1, 6, and 8 are displayed below the graph, propidium iodide - cyan, glutamine synthetase – blue, BrdU – red, scale bars

cells in the niche, including the delay or "gap" period from days 5-7, reflects the time required for cells in the source tissue to complete their lineages, be released, and travel to and incorporate into the niche (Benton et al., 2014).

Cells from the Immune System Generate Adult-Born Neurons in Crayfish

Recent work in the Beltz lab has outlined the functional relationship between the immune system and adult neurogenesis in crayfish (Benton et al., 2014). Unlike mammalian immune systems that are comprised of innate and adaptive responses, crayfish only possess an innate immune system in which hemocytes, or blood cells, are an integral player (Benton et al., 2014). There are two distinct tissues that form the crayfish immune system, the hematopoietic tissue (HPT) and the anterior proliferation center (APC), which generate hemocytes and release them into circulation (Noonin et al., 2012; da Silva et al., 2013). *In vitro* studies aimed at identifying the extrinsic source of the precursor cells examined the affinity of cells from various tissues for the niche, including green gland, hepatopancreas, hematopoietic tissue, and hemocytes (Benton et al., 2011). Of the tissues examined, hemocytes were strongly attracted to the niche and were the only cell type to demonstrate any such affinity. This result suggests that hemocytes produced by tissues from immune system may contribute the labeled NPCs appearing after the "gap" period.

To examine whether hemocytes contribute to the NPC population in the neurogenic niche *in vivo*, adoptive transfers were performed in which EdU-labeled blood cells were transferred from donors to live recipient crayfish *(P. clarkii*; Benton et al., 2014). EdU-labeled donor cells were subsequently found in the neurogenic niche of recipient crayfish, as well as integrated into the neuronal cell clusters 9 and 10, where they resembled neurons morphologically. Additionally, by seven weeks after the recipient was injected, the cells that had integrated into

the neural clusters expressed the expected neurotransmitters for the brain regions into which they had been incorporated (orcokinin in cluster 9 and SIFamide in cluster 10) (Benton et al., 2014). These experiments suggest that cells of the hematopoietic or immune system are competent to become neuronal precursor cells, and are a likely source of the NPCs involved in adult neurogenesis in crayfish.

Immune System-Brain Connections in Mammals

The involvement of the immune system in adult neurogenesis is not restricted to crayfish or invertebrates. In fact, there is a great deal of evidence suggesting that immune cells are capable of acting as neural precursors and giving rise to adult born neurons in mammalian species. Several studies in rodents have demonstrated that bone marrow may be induced to express electrophysiological neuronal properties in response to changes in the extracellular environment (Sanchez-Ramos et al., 1998; Sanchez-Ramos et al., 2000; Kohyama et al., 2001). Additionally, bone marrow cells and their derivatives are known to migrate to the brain and express neuronal markers (Kopen et al., 1999; Woodbury et al., 2000; Bonilla et al., 2002; Hess et al., 2002; Makar et al., 2002). Bone marrow cells have also been shown to express glial and neuronal genes (Goolsby et al., 2003). These findings in rodents are extended by two human studies in which bone marrow transplants from male donors were administered to female recipients. Cells that had the morphological and molecular characteristics of neurons and that carried the Y-chromosome were subsequently found in the brains of female recipients after death, further demonstrating the ability of bone marrow to migrate into the brain and differentiate into cells that have neuronal properties (Mezey and Chandross, 2000; Cogle et al., 2004).

However, many of these studies have been disputed, as some have argued that while bone marrow cells may have the ability to differentiate into neurons, this might not occur under normal physiological circumstances. Additionally, radiation is required in all mammalian studies of this nature, so that bone marrow transferred from one organism to another is not rejected. Some have proposed that this radiation may compromise the integrity of the blood brain barrier, allowing bone marrow cells to simply pass into the brain, a phenomenon that they argue would not occur in the absence of radiation (van Vulpen et al., 2002; Sirav and Seyhan, 2011). However, studies have demonstrated that mesenchymal stem cells, pluripotent stem cells found in adipose tissue, bone marrow, and blood, are able to cross the blood brain barrier under healthy conditions (Ruster et al., 2006; Steingen et al., 2008; Chamberlain et al., 2012). This evidence supports the possibility that immune-derived stem cells migrate to the adult mammalian brain where they may become neuronal precursors.

The Present Study: Research Aims and Significance

Current experiments in the Beltz lab are specifically focused on the immune system as a possible source of neuronal precursor cells in crayfish. Previous experiments have demonstrated that hemocytes act as neural precursors, giving rise to cells that morphologically and chemically resemble neurons and that integrate into clusters 9 and 10 (Benton et al., 2014). However, it is impossible to definitively state that these immune derived cells differentiate into functional neurons without electrophysiological data demonstrating that they share the electrical properties of neurons, which are integral to forming functioning neural connections. While nucleoside labels such as BrdU and EdU act as selective labels for immune-derived cells in adoptive transfer experiments (Benton et al., 2014), they can only be visualized after sacrifice of the animal and tissue fixation. This limitation makes it impossible to use these nucleoside labels as *in vivo*

markers, as would be necessary for determining the electrophysiological properties of immune derived cells in clusters 9 and 10.

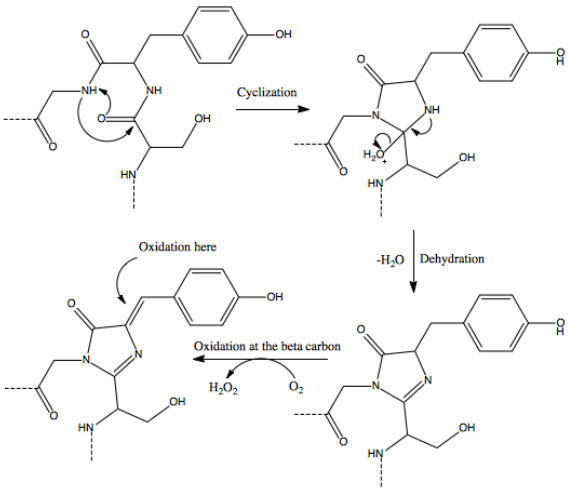

Figure 3. *Chemical mechanism of spontaneous cyclization of green fluorescent protein (GFP)*. This reaction results in the production of a highly conjugated system, causing the protein to have fluorescent properties.

The present study will examine whether the cells arising from blood-derived precursor cells in crayfish are fully functional neurons and form neural connections by using an *in vivo* marker, green fluorescent protein (GFP). GFP can be visualized *in vivo* with fluorescence microscopy, as it spontaneously cyclizes to form a highly conjugated molecule, providing a green fluorescent emission (Fig. 3). The present study aims to develop a transgenic crayfish that constitutively expresses green fluorescent protein (GFP) in all tissues, though most importantly in the hematopoietic tissues that generate blood cells. GFP-expressing blood cells will be adoptively transferred to recipients, and their progression followed as with the EdU-labeled cells used previously (Benton et al., 2014). The hypothesis is that the GFP-expressing blood cells will follow the same path described in Benton et al. (2014) and will be attracted to the niche, and generate a lineage of cells whose descendants will be located in brain clusters 9 and 10. However, the GFP expression will provide the means for examining the properties of immune-derived cells in the brain *in vivo*. Thus, the goal of this thesis project has been to generate crayfish that generate GFP-labeled (GFP+) blood cells. These transgenic crayfish will provide a

means for replicating the studies of Benton et al. (2014), and extending these to include electrophysiological analyses of GFP+ cells in brain clusters 9 and 10.

This thesis project describes two types of studies that were conducted with the final goal of doing electrophysiological studies of brain cells that are derived from adoptively transferred blood cells. The first study focuses on developing a GFP expressing crayfish by transfection with a lentiviral vector. Expression of GFP in the immune tissues will allow for immune-derived cells from GFP-expressing donors to be tracked *in vivo* within the brains of adoptive transfer recipients. Electrophysiological experiments may then be conducted on these cells to determine whether they have the same electrical properties as neurons and form functional neural connections. A dorsal approach has been established for electrophysiological studies of the crayfish brain (Sandeman et al., 2009). However, immune derived cells integrate into the brain ventrally through the neurogenic niche. Little is known regarding the timeline of cell movement from the ventral surface to the dorsal surface of the brain within cluster 10. In order to determine whether a dorsal approach may eventually be used for electrophysiological experiments or whether a new ventral approach must be developed, a second study was conducted in which the movement of newborn cells was tracked from ventral to dorsal regions of cluster 10. Together, these two studies lay the foundation for future electrophysiological examination of immune derived cells integrated into cluster 10 of the crayfish brain.

Materials and Methods

I. Animals: Experiments were conducted with either crayfish *Procambarus clarkii* or *Procambarus fallax*. Animals were maintained in the Wellesley College Animal Care Facility at room temperature on a 12/12 light/dark cycle. Aquariums contained artificial pond water consisting of double distilled water, trace minerals, and sodium bicarbonate.

II. Lentiviral Transfection: Transgenic GFP+ crayfish were developed by soaking the parthenogenic crayfish species *Procambarus fallax* in a lentiviral GFP vector during critical post-embryonic developmental stages. Using a parthenogenic (asexually reproducing) model is advantageous as GFP transfection may be passed down to future generations. The lentiviral particle achieves transfection by inserting its DNA into the DNA of cells it infects, so that the cells themselves transcribe and translate it along with their own DNA, in this case causing cells to produce GFP. The viral DNA is additionally replicated along with the host DNA during cellular division cycles, so that descendants of all transfected cells will also contain the GFP gene (Craigie and Bushman, 2012). The transduction particle is promoterless and is constitutively expressed once the vector has been incorporated (Sigma-Aldrich). Therefore, this particle is ideal for transfecting a wide range of cell types, including those in the immune tissues as well as hemocytes, and is appropriate for the present study.

Shortly after hatchlings separated from the mother, crayfish (*P. fallax*) were soaked in the Sigma MISSION TurboGFP Lentiviral Transduction Particles (Sigma Aldrich) for 10 hours at a concentration of 2:100 in crayfish saline (205 mM NaCl, 5.4 mM KCl, 34.3 mM $CaCl_2$, 1.2 mM $MgCl_2$, and 2.4mM $NaHCO_3$), and again during stages 4 and 5 of juvenile development (Figure 4; Vogt et al., 2004). These post-embryonic stages were strategically chosen in order to maximize probability of transfecting the ovaries and later developing a line of GFP transfected progeny. Transfection of immune tissues and hematopoietic cells was confirmed with confocal microscopy following either dissection of the HPT and APC or blood draws, in which 100-200ul of blood was drawn per animal and mounted on poly-L lysine treated slides. Tissues and blood samples were subsequently fixed with 4% paraformaldehyde in 0.1 phosphate buffer (PB; 20mM NaH_2PO_4, 80 mM Na_2HPO_4; pH 7.4) and processed with Hoechst (a nuclear stain). A subset of

hemocytes was additionally processed following standard immunohistochemical methods (see immunohistochemistry methods below) using an anti-GFP primary antibody.

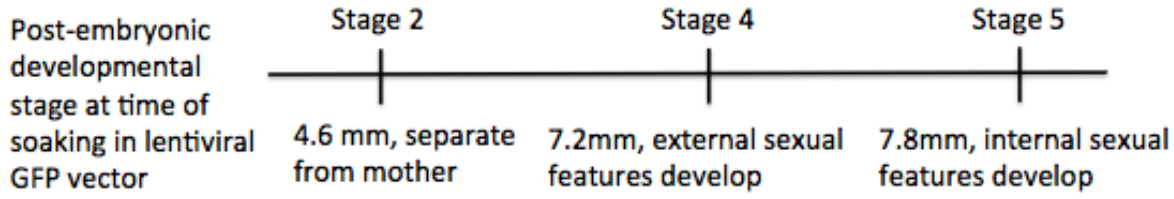

Figure 4. *Timeline of Procambarus fallax exposure to lentiviral GFP construct during post-embryonic development.* Animals were exposed to a lentiviral GFP vector at stages 2, 4, and 5 of post-embryonic development. Developmental stage was determined based on the length of the animal.

III. Confirmation of GFP Transfection Using Western Blot:

Tissue Homogenization and Protein Isolation: Tissues including brain, HPT, green gland, ovary, APC, and hepatopancreas were dissected from GFP-transfected *P. fallax* in crayfish saline. HPT and hepatopancreas were additionally dissected from control animals. Tissues were then homogenized in a 4^{o}C cold room with 1µl of protease inhibitor per 20mg of tissue in 500µl of homogenization buffer (10mM Tris(base), 10% glycerol, 400mM NaCl, 1mM DTT, 1mM EDTA, pH = 7.4 at 4^{o}C). Homogenates were centrifuged at 12,000 revolutions per minute at 4^{o}C for ten minutes, and the supernatants were collected and stored were stored at -80^{o}C.

Bradford Assay: Protein concentrations of homogenized tissue samples were quantified using the colorimetric Quickstart Bradford Protein Assay (BioRad). A 2mg/ml bovine serum albumin (BSA) standard was used, and was diluted to 1.5 mg/ml, 1 mg/ml, 750 ug/ml, 500 ug/ml, 250 ug/ml, and125 ug/ml in order to establish a standard curve for protein concentration. 20 uL of either standard or sample was combined with 1mL of ambient 1x Bradford Dye Reagent

(BioRad), and incubated at room temperature for at least five minutes and up to one hour. Absorbance of the standards and samples was then measured with a spectrophotometer at 595 nm. The spectrophotometer was first zeroed before reading with a blank sample containing homogenization buffer that had been incubated with the 1x Bradford dye. A standard curve was created by plotting the concentration of protein standards against their 595nm absorbance values. This curve was then used to determine the concentration of the protein samples.

Western Blot: Proteins from GFP transfected animals as well as controls were loaded into a NuPAGE protein gel (Thermofisher) secured in the buffer core filled completely with 1x Running Buffer (Thermofisher). The outer buffer chamber was filled 75% with 1x Running Buffer. As protein concentrations of the samples were very low, the maximum amount of protein possible was loaded per well from each tissue sample. From controls, 7.35 ug of HPT and 20.7 ug of hepatopancreas, and from GFP transfected animals, 24.4 ug of ovary, 26.38 ug of hepatopancreas, 5.72 ug of HPT, 2.99 ug of APC, and 6.98 ug of brain were loaded onto the gel. Additionally, 5 ul of rainbow kaleidoscope ladder (BioRad) was loaded. The gel was run at 100V for two hours.

A piece of PVDF membrane the size of the NuPAGE gel was incubated in methanol for two minutes, and then incubated in transfer buffer (1x NuPAGE transfer buffer, 1% methanol) for twenty minutes. After proteins were run, the gel was aligned with the PVDF membrane and assembled into an XCell blot module in transfer buffer, with two blotting pads and a piece of filter paper on either side of the gel and transfer membrane. The inner chamber of the blot module was filled with transfer buffer, and the outer chamber with deionized water. The transfer was then run at 30V for one hour.

Following transfer, the PVDF membrane was incubated for one hour at room temperature in 3% milk in tris-buffered saline (TBS), and then in 3% milk in tris-buffered saline with tween (TBST) and mouse anti-GFP (1:1000, Abcam) at 4^{o} overnight. The membrane was then rinsed three times for fifteen minutes in TBST and incubated for one hour at room temperature in Alexa fluor 488nm goat anti-mouse (1:2000, Jackson ImmunoResearch Laboratories). The membrane was subsequently rinsed in TBST for fifteen minutes, and quickly rinsed in water. The Western blot was imaged using a BioRad imager.

IV. Adoptive Transfers: Blood samples from GFP transfected *P. fallax* were examined for GFP expression prior to adoptive transfer. Blood draws were conducted with 25-gauge needles and 25 ul of anticoagulant buffer (AC buffer, 0.14M NaCl, 10mM EDTA, 30mM trisodium citrate, 26mM citric acid, 0.1M glucose, pH 4.6) was taken into the syringe before drawing blood. After removal, blood was immediately mixed with 50ul of AC buffer, and injected into the recipient crayfish (*P. fallax*) with a clean needle.

V. Quantitative Assessment of Newborn Cell Movement Throughout the Brain

EdU and BrdU injections: *P. Clarkii* were injected with either 5-bromo-2'deoxyuridine (BrdU; 0.5ml of 5mg/mL in crayfish saline) or 5-ethynyl-2'deoxyuridine (EdU; 0.5 mL of 0.02-0.2mg/mL in crayfish saline). *P. fallax* were injected with EdU.

Sectioning: Following BrdU or EdU injection, brains were dissected from injected *P. clarkii* at several time points: 4 (n=3), 6 (n=2), 8 (n=2), 10 (n=3), and 12 (n=2) weeks after injection, and from injected *P. fallax* at 7 weeks after injection (n = 2). Brains were fixed overnight in 4%

paraformaldehyde in 0.1 phosphate buffer. Tissues were subsequently sectioned at 100um with a Vibratome and processed with standard immunocytochemical (BrdU) and chemical (EdU) methods, as well as with Hoechst.

Cell Counts: The Leica Microsystems TCS SP5 microscope and Leica Microsystems LAS AF software (Leica Microsystems GmbH, Wetzlar, Germany) was used to visualize and count all cells labeled with either BrdU or EdU and Hoechst in cluster 10 of each brain section. Cells were counted by an individual observer. Sections were ordered from ventral to dorsal, and separate cell counts were conducted for the ventral, middle, and dorsal thirds of the brain in order to evaluate the movement of cells throughout cluster 10 as they differentiate. As individual animals undergo varying levels of cell proliferation, the number of cells counted in cluster 10 of each third of the brain were normalized and represented as percentages, so that data could be easily compared across animals. These percentages were calculated by counting the labeled cluster 10-cells within each third of the brain sections (ventral, middle, dorsal) and dividing these values by the total number of labeled cells in cluster 10. These data therefore indicated the proportion of labeled cells residing in each third of the brain for an individual animal.

VI. Immunohistochemistry: Immunohistochemical processing was conducted following standard procedures (Zhang et al., 2009). Tissues were rinsed several times with 0.3% Triton X-100 in PB (PBTx) for 1.5 hours (brains) or 15 minutes (blood cells), and incubated overnight in primary antibodies at 4^{o}C. Brains treated with BrdU were additionally incubated in 2NHCl for 45 minutes prior to treatment with primary antibodies. Samples were again rinsed in PBTx as previously indicated and incubated overnight in secondary antibodies and the nuclear stain

Hoechst (4',6-diamidino-2-phenylindole; Molecular Probes) in the dark at 4°C. Tissues were then rinsed with PB for 1.5 hours (brains) or 15 minutes (blood cells) and mounted with Fluoro-Gel (Electron Microscopy Sciences) for viewing and imaging with a Leica TCS SP confocal microscope and Leica Microsystems LAS AF software (Leica Microsystems GmbH, Wetzlar, Germany).

The following primary antibodies were used in the present study: rat anti-BrdU (1:50; Accurate Chemical) and mouse-anti GFP (1:100, Living Colors). The complementary secondary antibodies that were used (Jackson ImmunoResearch Laboratories) were goat anti-rat IgG-CY3, goat anti-mouse IgG-CY3, and goat anti-mouse IgG-CY5.

Results & Discussion

I. Generation of Transgenic *P. fallax* as blood donors for adoptive transfers

Results

A. Transfection of *P. fallax* with GFP

In order to transfect *P. fallax* with GFP, animals were exposed to a lentiviral GFP vector at key points during post-embryonic development. Immune tissues, including the HPT and APC, and hemocytes of transfected and control crayfish were subsequently examined with confocal microscopy at eight weeks to six months after initial exposure to the GFP lentiviral transduction particle in order to determine levels of GFP transfection. No fluorescence was observed in control tissues (Fig. 5 A, D, F). Cytoplasmic labeling in the GFP emission spectrum was observed in the HPT, the APC, and in hemocytes of transfected animals, suggesting successful GFP transfection (Fig. 5 B, C, E, G). However, the signal was weak and quickly degraded under laser excitation, and as a result, was difficult to image.

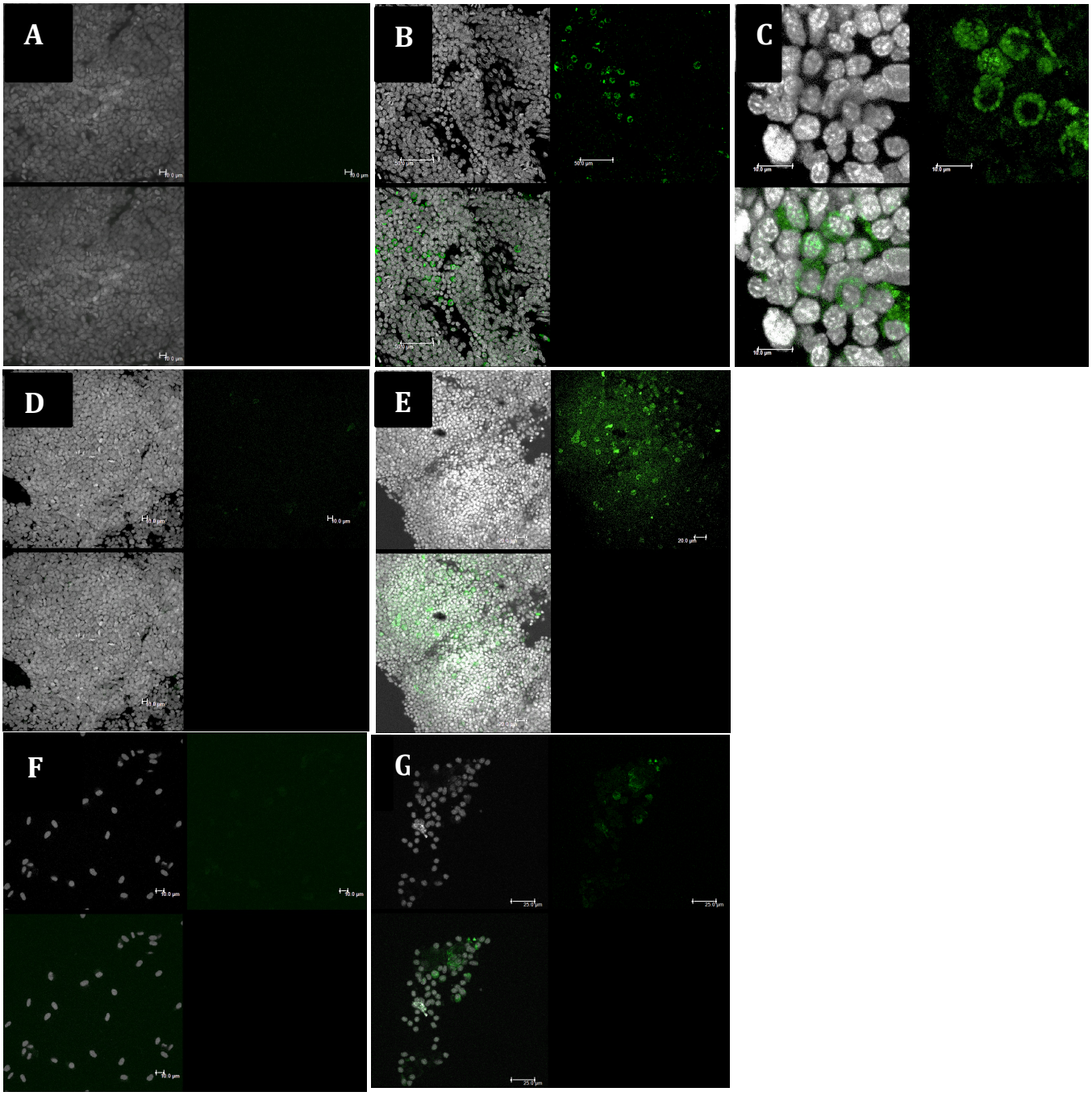

Figure 5. *Green fluorescent protein (GFP) expression in Procambarus fallax.* APC (A), HPT (D), and hemocytes (F) of control animals. GFP expression in the APC (B, C), HPT (E), and hemocytes (G) of *P. fallax,* eight weeks after exposure to lentiviral transduction particles *in vivo*. Signal intensity was maximized with the gain and offset settings on the microscope in order to illustrate the labeling. Green = GFP, Grey = Hoechst.

In order to evaluate the percentage of GFP+ hemocytes in transfected animals, a mouse anti-GFP primary antibody was used in conjunction with an Alexa 647nm-labeled goat anti-mouse secondary antibody to overcome the challenges that rapid signal degradation posed for counting cells. Hemocytes treated with this antibody appeared to have a very strong GFP signal that did not degrade throughout imaging on the confocal microscope (Fig. 6). Hemocytes from control animals were examined at the same time, and were not found to have any labeling in the GFP emission spectrum. Upon later examination, however, control samples had strong cytoplasmic fluorescent labeling in the green (488nm) emission spectrum, resembling labeling observed in transfected animals. The fluorescence observed in control hemocytes suggests that the confocal microscope was not functioning properly at the time control samples were originally examined.

An experiment was conducted in order to elucidate the source of the fluorescence in the 488nm (green) channel in control animals (not transfected with GFP). Blood samples were taken from control *P. fallax* and processed with three separate treatments, (1) Hoechst; (2) Hoechst and goat anti-mouse IgG-CY5 secondary antibody alone; and (3) Hoechst, mouse anti-GFP primary antibody, and goat anti-mouse IgG-CY5 secondary antibody, as was previously used to process hemocyte samples from GFP-transfected animals. Hemocytes were not found to fluoresce when treated with Hoechst alone (Fig. 7). However, when hemocytes were treated with Hoechst and secondary antibody, cells fluoresced in the far red (647nm), red (549nm), and green (488nm) emission spectra, despite the secondary antibody only providing a fluorescent tag in the far red range (Fig. 8). The same result was observed when hemocytes were treated with Hoechst, primary, and secondary antibodies (Fig. 9). When examined in the absence of cells, the secondary antibody alone did not cause fluorescence in any channel other than the appropriate

far-red range. Therefore, the secondary antibody is somehow inducing autofluorescence in hemocytes in channels where the fluorophore does not emit.

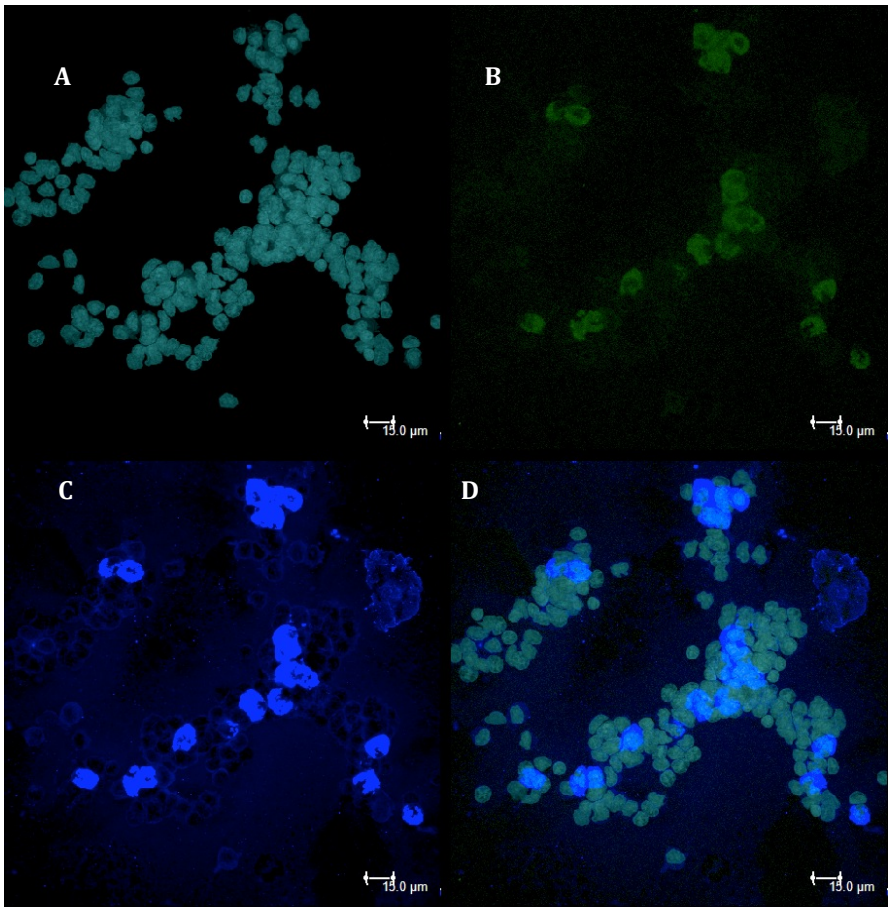

Figure 6. *Hemocytes from Procambarus fallax transfected with Green Fluorescent Protein (GFP), treated with antibodies*. Hemocytes were processed with Hoechst (A, cyan), mouse-anti GFP and goat anti-mouse IgG-CY5 (C, blue). (D) Overlay of panels A-C. Increased fluorescence compared with controls was observed in the 488nm emission spectrum (B, green). Smart gain 516 for Hoechst, 875 for 488nm, 484 for 647nm; smart offset consistently zero.

Additional secondary antibodies were examined in order to determine whether the observed autofluorescence effect could be induced by secondary antibodies in general, or whether it was specific to the goat anti-mouse IgG-CY5 secondary antibody used in these experiments. Hemocytes from *P. fallax* were processed with Hoechst and either goat anti-mouse IgG-CY2 or IgG-CY3 secondary antibody. Cells only fluoresced in the appropriate emission spectrum for the antibody used, indicating nonspecific antibody labeling of hemocytes. Unlike in previous studies employing goat anti-mouse IgG-CY5, cells did not fluoresce across emission spectra.

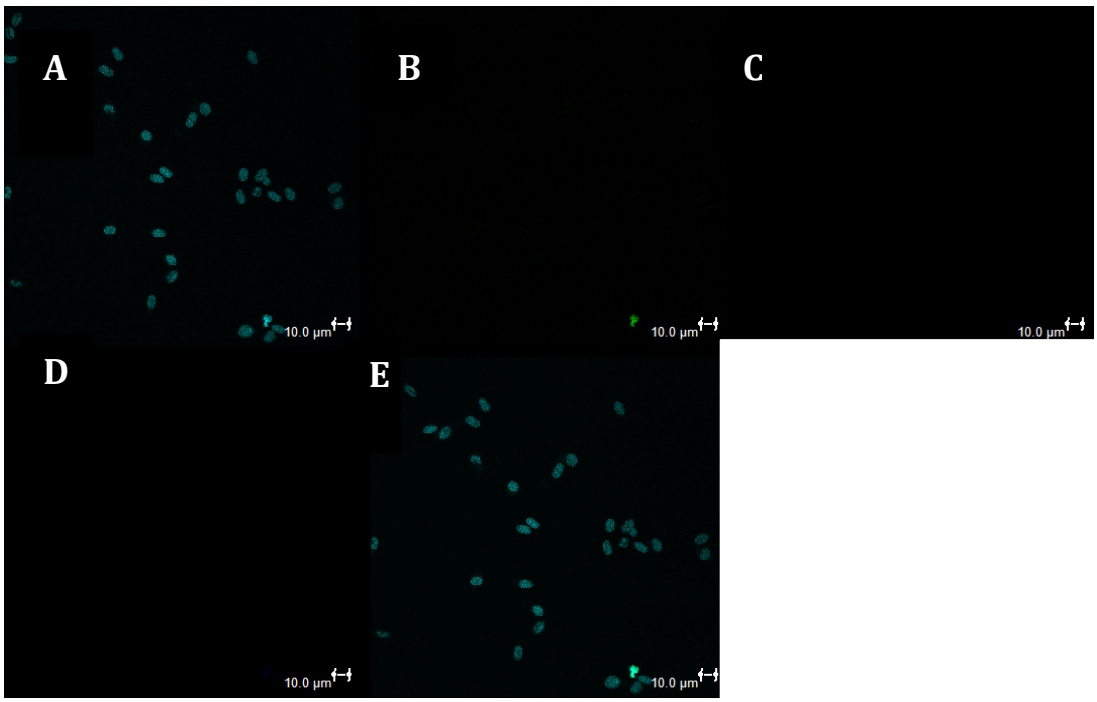

Figure 7. *Hemocytes from Procambaras fallax do not fluoresce in the 488nm, 594nm, or 647nm emission spectra when treated with Hoechst.* Hemocytes were treated with Hoechst and imaged with the confocal microscope. Cells appeared to only have a Hoechst label (A, Cyan). (B) 488nm (green) emission spectrum, (C) 594nm (red) emission spectrum, (D) 647nm (far red) emission spectrum, (E) overlay of panels A-D. The smart gain was 714 for Hoechst and 800 for all other emission spectra, and the smart offset was consistently zero.

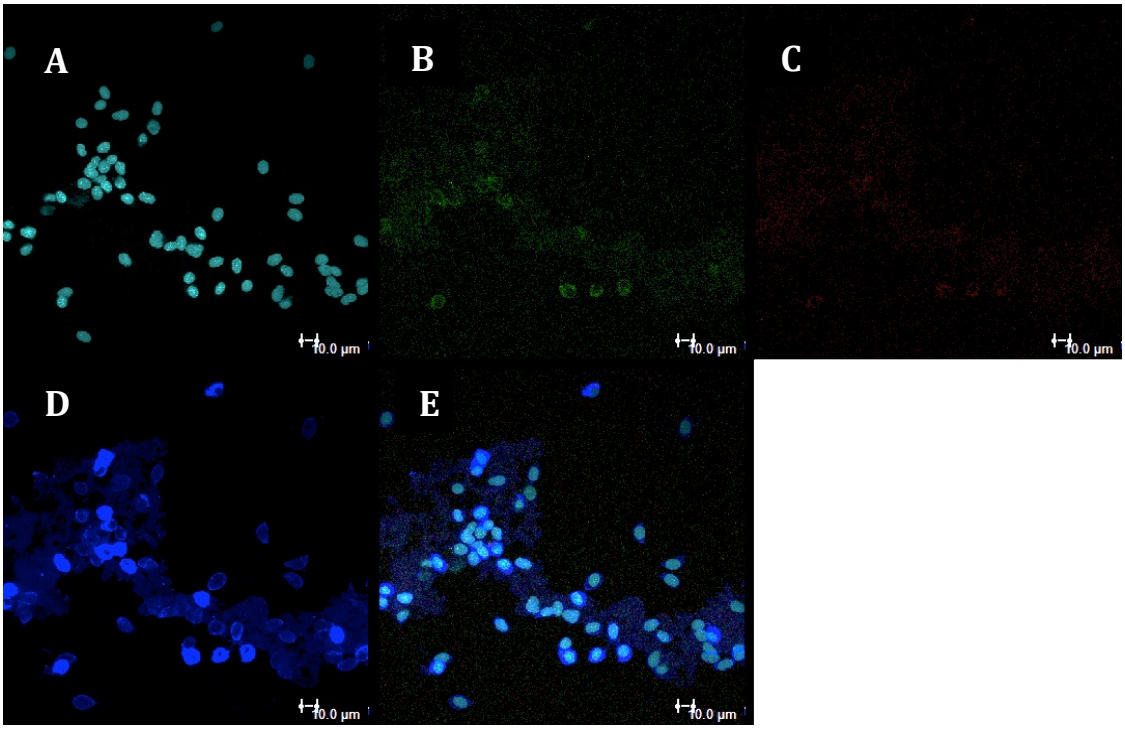

Figure 8. *Hemocytes from Procambaras fallax fluoresce in the 488nm, 594nm, and 647nm emission spectra when treated with Hoechst and goat anti-mouse IgG-CY5.* Hemocytes were processed and imaged with the confocal microscope. (A) Cells were labeled with Hoechst (Cyan). (B) Fluorescence was additionally observed in the 488nm

(green) emission spectrum, (C) the 594nm (red) emission spectrum, (D) and the 647nm (far red) emission spectrum (visualized in blue). (E) Overlay of panels A-D. The fluorescent signal in the 647nm emission spectrum is attributable to the IgG-CY5 secondary antibody. The smart gain was 714 for Hoechst and 800 for all other emission spectra, and the smart offset was consistently zero. While the signal in the 594nm emission spectrum is difficult to visualize, it is clearly visible on the confocal microscope.

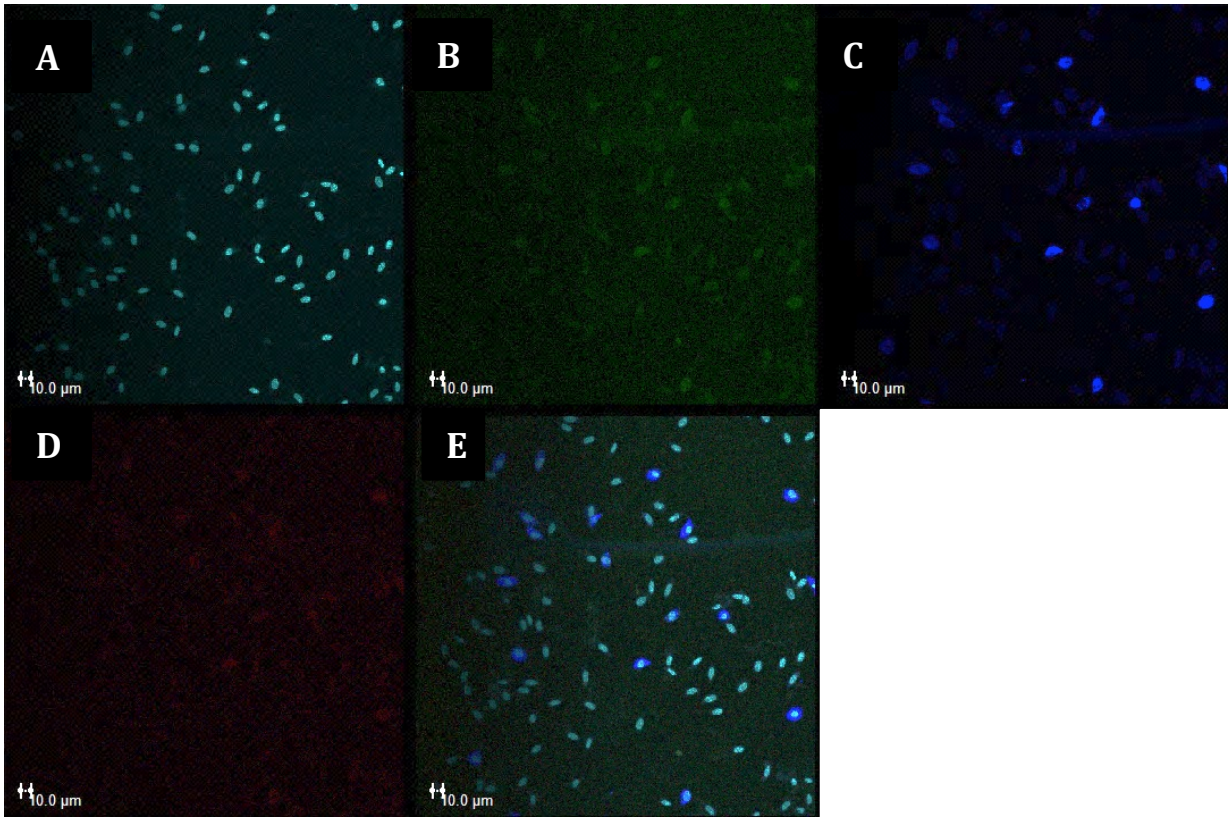

Figure 9. *Hemocytes from Procambaras fallax fluoresce in the 488nm, 594nm, and 647nm emission spectra when treated with Hoechst, mouse anti green fluorescent protein, and goat anti-mouse IgG-CY5.* Hemocytes were processed and imaged with the confocal microscope. (A) Cells were labeled with Hoechst (Cyan). (B) Fluorescence was additionally observed in the 488nm (green) emission spectrum (C) the 647nm (far red) emission spectrum, (D) and the 594nm (red) emission spectrum (visualized in blue). (E) Overlay of panels A-D. The fluorescent signal in the 647nm emission spectrum is attributable to the IgG-CY5 secondary antibody. The smart gain was 714 for Hoechst and 800 for all other emission spectra, and the smart offset was consistently zero. While the signal in the 594nm emission spectrum is difficult to visualize, it is clearly visible on the confocal microscope.

B. Western blots to confirm GFP expression.

Western blot was used to test whether the green cytoplasmic label originally observed on the confocal microscope in transfected animals was in fact due to GFP expression. Two separate Western blots were run. A Bradford Protein Assay was employed to determine the overall

protein concentration of tissue samples. For the first blot, the Bradford assay revealed very low protein concentrations in tissues homogenized from one animal, due to the small size of crayfish tissues. As a result, the amount of protein possible to run on a Western blot was far below the recommended value for all tissues except the ovaries. No GFP signal was observed on the blot using these samples. Therefore, for a second blot, tissues were pooled from four transfected animals. Protein concentrations remained low, however, for hepatopancreas and ovary, it was possible to load either 10 ug of protein or above per well, the minimum suggested protein mass to use in a Western blot. These two tissues from transfected animals were assayed, along with brain, HPT and APC, despite having less than 10ug of protein per well. Additionally, HPT and hepatopancreas were examined from control animals. No GFP was detected in either the tissues of control or GFP lentiviral treated animals (Figure 10).

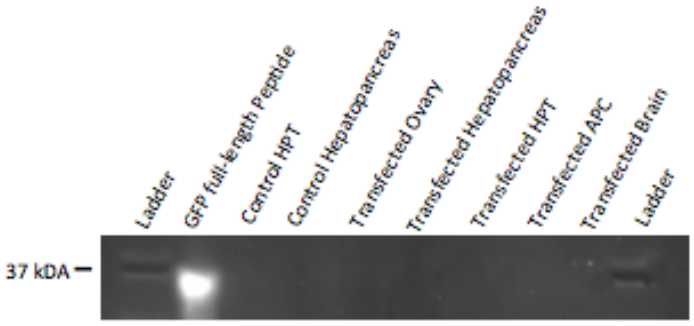

Figure 10. *Negative western blot evaluation of green fluorescent protein (GFP) expression in tissues from Procambarus fallax transfected with a GFP lentiviral vector and control tissues.* Western blot analysis shows that the GFP antibody recognizes the positive control full length GFP peptide at 39 kDa, but does not recognize protein from loaded samples.

C. Adoptive transfers using blood from GFP-transfected crayfish.

Several adoptive transfers were performed with hemocytes from GFP transfected *P. fallax*. Brains of recipients were examined with confocal microscopy three to four days after in order to determine whether GFP+ donor hemocytes had migrated to the niche or the streams. Fluorescent green cells were only observed near the niche in the brain of one recipient (Fig. 11).

Mouse anti-tyrosinated tubulin and goat-anti IgG-Cy5 were used to visualize the niche in adoptive transfers. As hemocytes labeled immunohistochemically with goat anti-mouse IgG-CY5 were found to fluoresce strongly in the 488nm emission spectrum (Fig. 8 and 9), it is possible that the signal observed in this experiment was caused by the same effect.

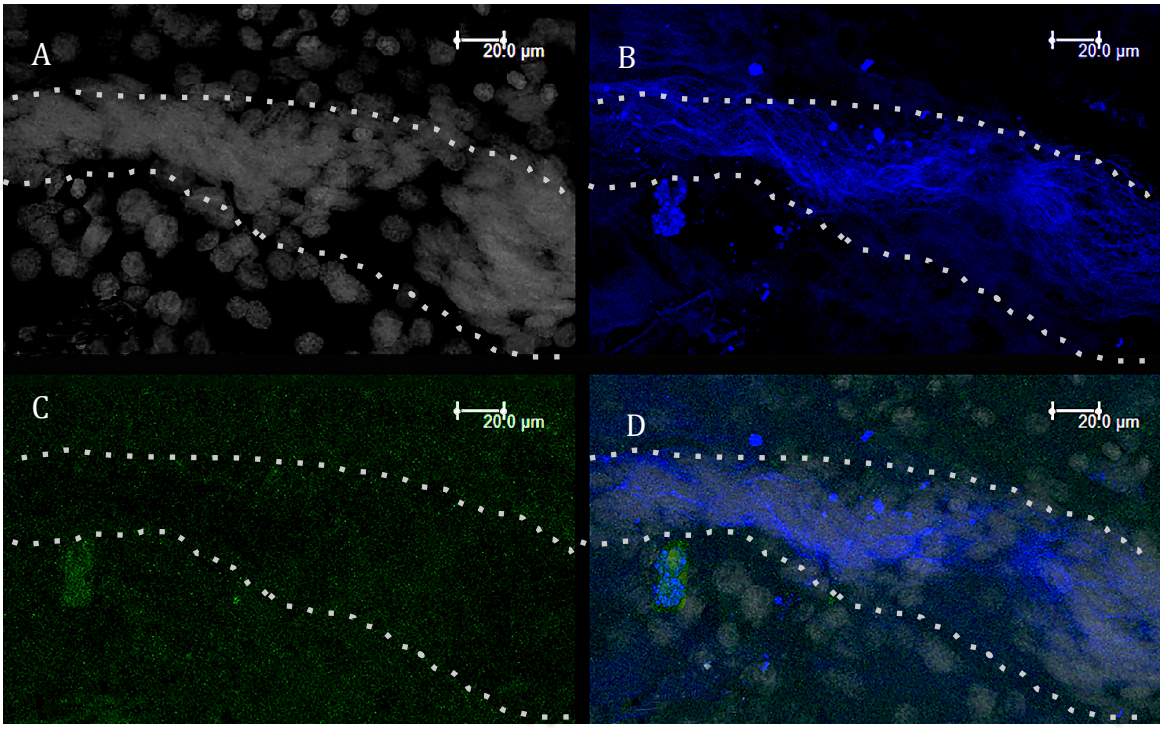

Figure 11. *Green fluorescently labeled cells observed near the niche in the brain of Procambarus fallax adoptive transfer recipient four days after injection with hemocytes from a green fluorescent protein (GFP) transfected donor.* The neurogenic niche is outlined in white. (A) Hoechst labeled cells (grey), (B) Anti-tyrosinated tubulin labeled cells (blue), (C) Green fluorescently labeled cells, (D) Overlay of panels A-C.

Discussion

A. Transfection of *P. fallax* with GFP

Green fluorescence in the immune tissues that give rise to hemocytes, as well as in hemocytes themselves, was observed in GFP transfected of *P. fallax* with confocal microscopy. GFP transfection was similarly achieved in cell cultures from Daphnia using a viral GFP vector (Robinson et al., 2006). However, the green signal observed in the present study is weak and

fades rapidly, and therefore is difficult to visualize. As a result, the established transfection method is likely not adequate to produce labeled cells that may be visualized clearly after adoptive transfer experiments for electrophysiology.

While employing an anti-GFP antibody in order to more easily quantify the percentage of GFP+ hemocytes in treated animals, fluorescence of hemocytes across several emission spectra was observed. Initially, in GFP-transfected hemocytes treated with only anti-GFP, the 488nm and 647nm emission spectra were examined, in which it was expected to observe GFP and anti-GFP signals, respectively. The 647nm-labeled secondary antibody was specifically chosen in the effort to avoid any signal overlap with green fluorescence, as its emission spectrum is the farthest from that of GFP. The fluorescence in the green range was very strong compared to the weak signal previously observed in tissues from transfected animals that had not been processed with antibodies. This increase in signal strength was interpreted as a sign of increasing GFP expression over time since initial transfection. While control samples initially appeared negative, later examination showed that these fluoresced identically to the hemocytes from experimental GFP-transfected animals, and were also found to fluoresce in the 594nm (red) emission spectrum. As this phenomenon also occurred in control animals upon treatment with 647nm-labeled goat-anti mouse secondary antibody in the absence of primary antibody, and did not occur when cells were treated with Hoechst alone, it is likely that treatment with the 647nm-labeled goat-anti mouse secondary antibody triggers autofluorescence in hemocytes. When examined in the absence of cells, the secondary antibody did not did not generate a fluorescent signal in any channel other than the appropriate emission wavelength. This result suggests that the fluorescence observed in these antibody-treated hemocytes was not due to a bleed-through effect of the antibody alone, and further supports the hypothesis that hemocyte autofluorescence

was inducted in the presence of the secondary antibody used. The mechanism of this autofluorescence and how it may be triggered by the secondary antibody employed is unknown. Other secondary antibodies were tested as additional controls for this problem, and treated hemocytes only fluoresced in the emission spectrum associated with the secondary antibody employed and did not fluoresce across several emission spectra. Therefore, the autofluorescence observed is not induced by all secondary antibodies, and may be specific to the goat anti-mouse IgG CY5 antibody used. In order to avoid this problem in future experiments, different antibodies should be used instead of the goat anti-mouse IgG CY5 from Jackson ImmunoResearch Laboratories for immunohistochemical processing of tissues.

Unfortunately, due to malfunctions with the confocal microscope at the time of examining control hemocytes, the strong signal in the green emission spectrum caused by autofluorescence was mistaken for a strong GFP signal in the transfected animals. While weak transfection had previously been achieved, this strong signal appeared encouraging for future experiments. As a result, efforts were focused on pursuing adoptive transfer experiments with GFP+ hemocytes instead of improving transfection methods. However, current experiments are examining ways in which to increase GFP transfection in order to produce a cellular label that may be easily visualized *in vivo*.

B. Western blots to confirm GFP expression.

Western blot was conducted as a molecular confirmation of GFP expression in transfected animals. It is important to note that Western blot was not used to examine expression of GFP in hemocytes, but rather in hepatopancreas, ovary, brain, and the immune tissues (HPT and APC). No tissues other than blood cells in the crayfish appear to undergo autofluorescence

or to consistently non-specifically label in the presence of secondary antibody, as extensive work in the Beltz lab has been performed using immunohistochemistry on various tissues and, excluding hemocytes, no such fluorescence has been observed in the past. Additionally, in preparing samples for Western blot, cell contents are separated with centrifugation prior to loading the gel in order to isolate protein from insoluble cellular materials. As a result, cell contents that may autofluoresce or routinely non-specifically label after immunohistochemical processing (e.g. granules) may have been removed from samples. Furthermore, goat anti-mouse IgG CY2 secondary antibody was used to visualize bands in the Western blot, which did not cause any autofluorescent effects across emission spectra in hemocytes. Therefore although Western blot, an antibody-based assay, was used to evaluate GFP expression, the results were likely not compromised by autofluorescent effects caused by processing with secondary antibody.

While no GFP was detected by Western blot in the tissues examined, this is not necessarily indicative of failed transfection. Low amounts of protein were loaded onto the Western gel due to the small size of crayfish tissues, despite pooling samples from multiple animals. It is suggested to load between 10 and 50 ug of protein onto a Western gel (Novus-Biologicals, 2015). While 20 ug of protein from the hepatopancreas and 26ug from the ovaries were assayed, the amount of protein loaded may still have been increased up to 50 ug, the maximum suggested mass of protein to load onto a Western gel, and expression possibly detected. Below 10 ug of brain, HPT and APC were loaded onto the gel, and were thus below the standard amount of protein suggested for this assay. Additionally, the cytoplasmic label in the GFP emission spectrum observed on the confocal microscope was very weak, suggesting that GFP expression is low and likely difficult to detect, even with Western blot. Furthermore, only a

fraction of cells in transfected tissues were observed to express GFP on the confocal microscope, likely increasing the difficulty of detecting the already-weak signal. It is likely that if GFP is weakly expressed, it makes up a very small portion of the overall protein measured in each sample. While it is possible that the negative Western result may truly indicate an absence of GFP, it is also very possible that the GFP concentration was much too low to be detected with this method.

C. Adoptive transfers using blood from GFP-transfected crayfish.

Several adoptive transfers were conducted with hemocytes from GFP-transfected donors, and labeled cells were only found near the niche in the brain of one recipient. This number is alarmingly low, as previous studies have observed BrdU labeled donor hemocytes in the niches of thirty percent of recipients (J Benton, personal communication). These transfers were performed prior to discovering that the GFP label observed on the confocal microscope in cells treated with anti-GFP antibodies was artifact, and that the signal was in fact much weaker than previously thought. The absence of GFP+ cells observed in the brains of recipients may therefore be due to a weak and rapidly degrading GFP signal, rather than an inability of donor hemocytes to migrate to the niche.

In the case of the one recipient in which labeled cells were observed near the niche, it cannot be determined whether the green fluorescent signal was truly a GFP+ cell, or whether it was artifact, as mouse anti-tyrosinated tubulin and goat anti-mouse IgG-CY5 antibodies were used in order to visualize the niche. This adoptive transfer was performed before the 647nm-labeled goat-anti mouse was discovered to cause fluorescence of hemocytes across emission spectra. As a result, the 594nm emission spectrum was not evaluated, which may have provided insight as to whether the secondary antibody triggered fluorescence of hemocytes in this case. In

future adoptive transfer experiments, the goat anti-mouse IgG-CY5 secondary antibody from Jackson ImmunoResearch Laboratories should be avoided to reduce the possibility of hemocytes autofluorescing, and other antibodies should be used to visualize the niche.

II. Quantitative Assessment of Newborn Cell Movement Throughout the Brain

Results

Nucleoside-labeled cells were tracked in the cluster 10 of the *P. clarkii* brain, in order to establish a timeline of cell movement for newly born neurons. These data will serve as a basis for electrophysiological examination of adult-born neurons derived from the adoptive transfer of GFP+ blood cells. As neurons initially incorporate into the ventral surface of the brain near the site where the migratory streams end and then move dorsally, newborn cells were counted in cluster 10 from the ventral to the dorsal surface, to determine at what point a sizable population of labeled cells may be found in the dorsal third of the brain. As standard brain preparations used for electrophysiology expose the dorsal surface of the brain and are perfused through the dorsal artery, it is important to know at what time-point transferred cells may be expected to reside dorsally (Sandeman et al., 2009).

Brains were examined 4, 6, 8, 10, and 12 weeks after injection with either BrdU or EdU (Fig. 12). At four weeks after injection, the majority of labeled cells reside in the ventral and middle thirds of the brain, and few cells in the dorsal third. By six weeks after injection, cells appear to have moved more dorsally, as the majority of labeled cells were found in the middle third of the brain rather than the ventral third. At eight weeks post-injection, cells are approximately evenly split across the brain, with an average of 32% of cells in the ventral third, 31% of cells in the middle, and 36% of cells in the dorsal third for all animals examined (n=2).

Importantly, the average percentage of cells in the dorsal third remains relatively stable throughout weeks ten to twelve for all animals assessed at each time point, as does the general distribution of cells throughout the remainder of the brain. In animals examined at ten weeks, on average 47% of labeled cells reside in the ventral third, 24% in the middle, and 28% in the dorsal third (n=3). In animals assessed at twelve weeks, an average of 38 % of labeled cells were found in the ventral third, 25% in the middle, and 36% in the dorsal third (n=2). Therefore, a few dorsally-located labeled cells can be found as early as week 4 post-injection in some animals, but these are not found consistently until later time points. However, by eight weeks post injection of a mitotic marker, a relatively stable proportion of cells inhabit the dorsal third of the brain in *P. clarkii*.

In order to determine whether cells newly incorporated into the brain reach a similar migratory distribution in *P. fallax*, the species being used for transfection, cell movement was examined seven weeks following BrdU injection in two animals. The full study (as above in *P.* clarkii) was not conducted in *P. fallax* because this colony of crayfish has limited numbers of animals that are needed for many types of studies, and this species cannot be acquired from commercial vendors. As *P. fallax* appear to develop more rapidly than *P. clarkii*, it was hypothesized that cells may reach the relatively stable distribution observed at eight weeks in *P. clarkii* sooner, and thus cell movement was evaluated seven weeks after injection. A sizable portion of cells were found in the dorsal third of the brain, and cells appeared to be well distributed with on average 42% of labeled cells in the ventral third, 22% of cells in the middle, and 35% of cells in the dorsal third. By seven weeks, labeled cells in *P. fallax* seem to have reached a distribution very similar to the stable distribution observed by eight weeks in *P. clarkii.*

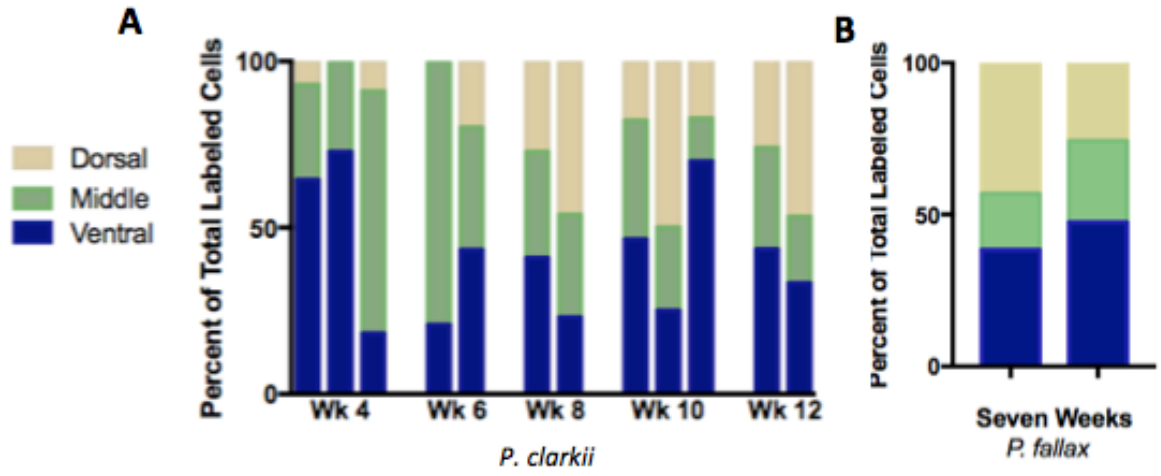

Figure 12. *Dorsal Movement of BrdU or EdU labeled cells after incorporation into Cluster 10.* (A) *Procambarus clarkii* were injected with EdU or BrdU, and at 4 (n=3), 6 (n=2), 8 (n=2), 10 (n=3), and 12 (n=2) weeks post injections. (B) *Procambarus fallax* were injected with EdU (n=2) and at 7 weeks post injections. All brains were assessed for how far dorsally EdU or BrdU labeled cells moved through cluster 10. Each bar represents the total EdU or BrdU labeled cells in cluster 10 of one animal.

Discussion

The positions of newly integrated cells throughout cluster 10 in the brain were evaluated in order to determine the timeline during which neurons move from the ventral region of brain cluster 10 where the migratory streams insert to more dorsal regions. Past electrophysiological techniques have recorded from cells on the dorsal surface of the brain. However, this may pose a problem in experiments examining the electrophysiological properties of newborn neurons that incorporate into the brain ventrally, as will be the case in future adoptive transfer experiments that will be conducted with GFP+ hemocytes. It is therefore important to know at what time-point labeled cells reach the dorsal surface, if established electrophysiological protocols are to be employed. In *P. clarkii*, 36% of labeled cells were found to move to the dorsal third of the brain after eight weeks. Furthermore, this population in the dorsal region of the brain remained relatively stable through to twelve weeks, the final time point examined. These results suggest that by eight weeks, a sizable proportion of cells move from the ventral surface of the brain to

the dorsal surface, and that electrophysiological experiments with a dorsal approach may be conducted at that time. As current experiments focusing on GFP+ hemocytes are being conducted in *P. fallax*, it is important to determine whether cells follow the same movement pattern and timeline as in *P. clarkii*. As cells in *P. fallax* examined at seven weeks after BrdU injection reached a similar distribution throughout the brain to cells observed in *P. clarkii* at eight weeks with 35% of cells residing in the dorsal third of the brain, experiments utilizing a dorsal approach may be conducted on *P. fallax* as early as seven weeks after adoptive transfers.

Electrophysiological studies assessing whether GFP+ immune derived cells in the brain form neural connections must be conducted after cells have differentiated to anatomically and chemically to resemble neurons. By three weeks post-BrdU injection, BrdU-labeled cells demonstrate anatomical neuronal differentiation, and by eight weeks post-injection, a stable population of BrdU-labeled cells in cluster10 expresses SIFamide, a neurotransmitter that is found in the majority of cluster 10 cells (Schmidt and Demuth, 1998; Kim et al., 2014). Therefore, electrophysiological studies on GFP+ cluster 10 cells may be conducted eight weeks after adoptive transfers. By this time-point, a stable and sizable population of labeled cells may be expected to reside in the dorsal third of the brain, and thus, eight weeks or later after adoptive transfer of hemocytes will be the optimal time for electrophysiological experiments to be conducted.

Future Directions

The present studies have established a method for GFP transfection of *P. fallax* with a lentiviral vector and assessed the timeline of newborn cell movement from the ventral to dorsal regions of cluster 10, creating a foundation for future electrophysiological examination of immune-derived cells in the crayfish brain. In the first study, a method for transfection was

developed and GFP+ cells in HPT, and APC, and hemocytes were observed with confocal microscopy in animals exposed to the lentiviral vector early in post-embryonic development with confocal microscopy. This GFP signal was weak and quickly degraded in the majority of animals. Western blot did not confirm GFP expression in these crayfish tissues, which may have been due to low protein concentrations. In the second study, a timeline of newborn cell movement within cluster 10 was established which indicated that a stable population of cells is found in the dorsal region of cluster 10 by 7-8 weeks following BrdU-labeling in *P. clarkii* and *P. fallax*. These data suggest that electrophysiological studies using the standard dorsal approach (e.g., Sandeman et al., 2009) can be conducted following this time-point with the expectation that cells derived from adoptive transfers would have reached the dorsal regions of cluster 10.

Current experiments are evaluating whether GFP transfection was truly achieved using polymerase chain reaction (PCR) and gel electrophoresis. This method is much more sensitive than Western blot, as only one copy of the GFP vector must be incorporated into the DNA for it to be amplified by PCR and detected on a gel. As a result, PCR will give a clear indication as to whether the GFP vector has been successfully transfected into animals. If a positive result is attained, future efforts will be focused on increasing GFP transfection and maximizing expression.

It is unknown whether GFP expression with the established transfection method, if confirmed by PCR, is weak due to insufficient copies of the vector incorporating into the host DNA, or whether it is due to low levels of expression following incorporation. In order to address these possibilities and improve GFP transfection, *in vitro* experiments are being conducted by Kara Banson in the Beltz lab that aim to increase vector incorporation as well as protein expression. It is advantageous to conduct trials *in vitro,* as results can be quickly

observed and methods subsequently altered without having to wait several months for animals to fully develop before assessing transfection efficacy, as is the case in whole-animal transfection. Studies have demonstrated that incubating cells in histone 2A, which has DNA delivery activity, can improve the efficiency of lentiviral transfection by increasing the number of copies of DNA incorporated into host DNA (Liu and Soderhall, 2006). Using Histone 2A will not likely prove successful for *in vivo* whole-animal transfection, as it may be difficult to effectively inject animals with the protein and ensure that it effectively reaches the immune tissues. However, cells used in adoptive transfers need not come from live animals, and labeled cells generated in cell cultures may instead be injected into recipient crayfish. Thus, using histone 2A to transfect cells in culture with GFP will potentially provide the labeled cells necessary to perform future adoptive transfer experiments in order to generate newborn neurons in recipient crayfish for electrophysiological analysis.

It is possible that the weak GFP signal observed is also due in part to low GFP expression levels after transfection. The Woodchuck Hepatitis Post Transcriptional Regulatory Element (WPRE) has been demonstrated to increase expression of lentiviral transgenes by increasing the number of mRNA transcripts exported from the nucleus (Zufferey et al., 1999). In order to improve GFP expression, a WPRE vector will be introduced in conjunction with the lentiviral GFP vector. This combination of vectors may be used either in whole-animal transfection or to transfect cells in culture that may then be used for adoptive transfer experiments.

In future studies, transgenic crayfish expressing GFP will be used as hemocyte donors to repeat the adoptive transfer experiments performed by Benton et al. (2014). The use of GFP as a marker will allow for the movement of donor cells to be tracked in the living tissues of GFP naïve recipients without requiring animal sacrifice, immunohistochemical processing, and

fixation to view labeling, as is necessary with nucleoside labels. Additionally, as GFP will be expressed in donor cells and their descendants, cells arising from donor lineages within the recipient will retain the GFP label. It will therefore be possible to visualize GFP+ immune derived cells integrated into clusters 9 and 10 in the brains of recipient crayfish *in vivo,* and to perform electrophysiological experiments to determine whether these cells create functional synapses and acquire the electrical properties of fully functioning neurons. Future evaluation of electrophysiological properties will be conducted by comparing activity patterns of GFP+ descendants of donor cells with nearby mature neurons native to the recipient's brain. Furthermore, as GFP is expressed throughout the entire cell, the morphology of the GFP+ cells can be visualized, and it may be determined whether labeled cells project to and innervate normal targets in the recipient crayfish.

The functionality of new neurons born into the adult mammalian hippocampus was examined in a similar study, conducted by van Praag et al. (2002). This study used a retroviral GFP vector which labeled dividing cells, and therefore was expressed in all newborn neurons, making it possible to visualize them in *vivo*. The authors performed electrophysiological recordings of GFP+ neurons in live hippocampal slices and compared results to recordings from mature hippocampal neurons. To assess the ability of cells to fire action potentials, action potential thresholds of GFP+ cells were evaluated. To assess whether GFP+ cells had functional inputs, spontaneous postsynaptic currents were recorded, which also allowed the authors to assess whether neurons were receiving excitatory or inhibitory inputs. To evaluate whether new neurons receive appropriate projections, postsynaptic recordings were measured in response to extracellular stimulation of the perforant path. Passive membrane properties were also evaluated, including capacitance, time constant τ_m, voltage, and resistance.

Future studies will evaluate newborn GFP+ immune-derived cells in clusters 9 and 10 using methods similar to van Praag et al. (2002). The same electrophysiological properties that were evaluated by van Praag et al. (2002) will be evaluated in GFP+ cells in the crayfish brain, and compared to those of mature resident cells in the same cluster. Additionally, the morphology of GFP+ cells will be evaluated, as well the ability of these cells to form synapses, which will be determined using immunohistochemistry. As newborn neurons demonstrate different electrophysiological properties from mature neurons (van Praag et al., 2002; Schmidt-Hieber et al., 2004), electrophysiological recordings will be conducted at different time points following adoptive transfers, to determine whether the immune-derived GFP+ cells experience the same maturation patterns that are observed in adult mammalian neurogenesis.

Appendix A: Method for Quantifying Percentage of GFP Labeled Hemocytes

A method was developed for quantifying the percentage of GFP+ hemocytes in GFP transfected *P. fallax* in order to determine transfection efficacy. Due to weak signal and rapid degradation, anti-GFP was used to easily visualize and count GFP+ cells. However, as the antibody was later discovered to cause non-specific autofluorescence in some hemocytes, the calculated percentages of labeled blood cells became invalid. However, the method established to determine the percentage of labeled cells will prove useful for future counting experiments.

Blood samples were imaged on the confocal microscope, and six distinct regions on the slide were photographed per sample. Regions were selected for imaging based solely on high cell density, determined by Hoechst labeling. Following imaging, counting was conducted by a blinded individual. The total number of Hoechst labeled cells per image as well as the number of cells with cytoplasmic green fluorescent labeling were tabulated. The percentage of green fluorescently labeled cells was calculated by dividing the total number of fluorescent cells by the total number of Hoechst labeled cells. The percentage of green fluorescently labeled cells was averaged across all six frames photographed per blood sample, yielding an average percentage of labeled hemocytes per animal. This method may be improved by increasing the number of frames imaged per sample to increase accuracy by expanding the sample size.

Appendix B: Protein Concentrations of Tissue Homogenates Determined by the Bradford Assay

Western blots were run with tissues from transfected *P. fallax* in order to confirm GFP expression. A Bradford assay was first used to determine the protein concentration of tissue samples. The first Western blot that was run was loaded with protein from an individual transfected animal and an individual control. The Bradford assay revealed low protein concentrations for the majority of these homogenates (Table 1).

Due to the extremely low protein concentrations in the first Western blot, a second western blot was performed with protein samples pooled from four animals. The Bradford assay revealed higher protein concentrations in the pooled samples compared to samples collected from individual animals (Table 2). However, protein concentrations remained relatively low for the purpose of Western blot.

Treatment	Tissue	Protein Concentration (ug/mL)
GFP Transfected	Hepatopancreas	349.3
	Ovary	2234.3
	HPT	439.3
	APC	2.99
	Brain	176
	Green Gland	112.6
Control	HPT	5.55
	Hepatopancreas	744.89

Table 1. *Protein concentrations of Procambaras fallax tissue homogenates determined by Bradford Assay*. Tissues were dissected and homogenized either from one GFP transfected animal or from one control. Protein concentrations were determined by Bradford assay, and are indicated in ug/mL.

Treatment	Tissue	Protein Concentration (ug/mL)
GFP Transfected	Ovary	2440.75
	Hepatopancreas	2637.83
	HPT	572
	APC	298.87
	Brain	697.6
Control	HPT	734.5
	Hepatopancreas	2070.75

Table 2. *Protein concentrations of pooled Procambaras fallax tissue homogenates determined by Bradford Assay*. Tissues were dissected and homogenized from either four GFP transfected animals or from four control. Protein concentrations were determined by Bradford assay, and are indicated in ug/mL.

Appendix C: Determining the Amount GFP Full-Length Peptide to Run on Western Blot

A bright band on a western blot may overpower more subtle bands or make the gel difficult to image. In order to ensure that the recombinant full-length GFP peptide that was used as a positive control would not overpower potential experimental results, a Western blot was run with different amounts GFP loaded per well, ranging from 2000-12.5 ng (Fig. 13). 800ng of peptide loaded onto the gel produced a distinctly visible signal that was not overwhelming. This amount of peptide was thus used to run the first Western blot examining GFP transfected tissues. However, due to the lack of GFP expression in experimental and control samples, 800ug of the full-length GFP peptide appeared overly powerful. As a result, the amount of peptide loaded onto the second experimental Western blot was reduced to 600ug.

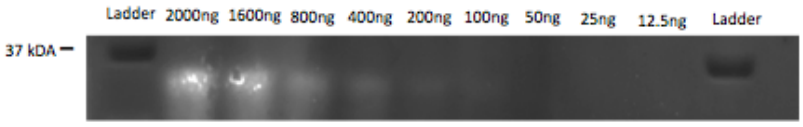

Figure 13**.** *Evaluation of signal strength for a range of 2000-12.5ng of GFP full-length peptide loaded in a Western blot.* Western blot analysis shows that the GFP antibody recognizes the full length GFP peptide at 39 kDa.

References

Altman J, Das GD (1965) Autoradiographic and histological evidence of postnatal hippocampal neurogenesis in rats. The Journal of comparative neurology 124:319-335.

Ayub N, Benton JL, Zhang Y, Beltz BS (2011) Environmental enrichment influences neuronal stem cells in the adult crayfish brain. Developmental neurobiology 71:351-361.

Bear MF, Connors BW, Paradiso MA (2007) Neuroscience: Exploring the Brain, III Edition. Baltimore, MD: Lippincott Williams & Wilkins.

Bédard A, M C, Lévesque M, Parent A (2002) Proliferating cells can differentiate into neurons in the striatum of normal adult monkey. Neuroscience Letters 3:213-216.

Beltz BS, Zhang Y, Benton JL, Sandeman DC (2011) Adult neurogenesis in the decapod crustacean brain: a hematopoietic connection? The European journal of neuroscience 34:870-883.

Benton J, Chaves da Silva P, Sandeman D, Beltz B (2013) First-generation neuronal precursors in the crayfish brain are not self-renewing. International Journal of Developmental Neuroscience 31:657-666.

Benton J, Kery R, Li J, Noonin C, Soderhall I, Beltz B (2014) Cells from the innate immune system generate adult born neurons in crayfish. Developmental Cell 30:332-333.

Benton JL, Zhang Y, Kirkhart CR, Sandeman DC, Beltz BS (2011) Primary neuronal precursors in adult crayfish brain: replenishment from a non-neuronal source. BMC neuroscience 12:53.

Bonilla S, Alarcon P, Villaverde R, Aparicio P (2002) Hematopoietic progenitor cells from adult bone marrow differentiate into cells that express oligodendroglial antigens in the neonatal mouse brain. European Journal of Neuroscience 15:575-582.

Calzolari F, Michel J, Baumgart EV, Theis F, Gotz M, Ninkovic J (2015) Fast clonal expansion and limited neural stem cell self-renewal in the adult subependymal zone. Nat Neurosci 18:490-492.

Cameron HA, Woolley CS, McEwen BS, Gould E (1993) Differentiation of newly born neurons and glia in the dentate gyrus of the adult rat. Neuroscience 56:337-344.

Cedar H, Kandel E, Schwartz J (1972) Cyclic Adenosine Monophosphate in the Nervous System of Aplysia Californica. I. Increased Synthesis in Response to Synaptic Stimulation. Journal of General Physiology 5:558-569.

Chamberlain MD, Gupta R, Sefton MV (2012) Bone marrow-derived mesenchymal stromal cells enhance chimeric vessel development driven by endothelial cell-coated microtissues. Tissue Eng Part A 18:285-294.

Cogle CR, Yachnis AT, Laywell ED, Zander DS, Wingard JR, Steindler DA, Scott EW (2004) Bone marrow transdifferentiation in brain after transplantation: a retrospective study. Lancet 363:1432-1437.

Craigie R, Bushman FD (2012) HIV DNA Integration. Cold Spring Harbor Perspectives in Medicine 2.

da Silva PGC, Benton JL, Sandeman DC, Beltz BS (2013) Adult Neurogenesis in the Crayfish Brain: The Hematopoietic Anterior Proliferation Center Has Direct Access to the Brain and Stem Cell Niche. Stem Cells and Development 22:1027-1041.

Dirks PB (2010) Brain tumor stem cells: the cancer stem cell hypothesis writ large. Molecular oncology 4:420-430.

Doetsch F, Garcia-Verdugo JM, Alvarez-Buylla A (1997) Cellular composition and three-dimensional organization of the subventricular germinal zone in the adult mammalian brain. J Neurosci 17:5046-5061.
Encinas JM, Michurina TV, Peunova N, Park JH, Tordo J, Peterson DA, Fishell G, Koulakov A, Enikolopov G (2011) Division-coupled astrocytic differentiation and age-related depletion of neural stem cells in the adult hippocampus. Cell Stem Cell 8:566-579.
Eriksson PS, Perfilieva E, Bjork-Eriksson T, Alborn AM, Nordborg C, Peterson DA, Gage FH (1998) Neurogenesis in the adult human hippocampus. Nature medicine 4:1313-1317.
Fuentealba LC, Rompani SB, Parraguez JI, Obernier K, Romero R, Cepko CL, Alvarez-Buylla A (2015) Embryonic Origin of Postnatal Neural Stem Cells. Cell 161:1644-1655.
Garcia-Verdugo JM, Ferron S, Flames N, Collado L, Desfilis E, Font E (2002) The proliferative ventricular zone in adult vertebrates: A comparative study using reptiles, birds, and mammals. Brain Research Bulletin 57:765-775.
Germano I, Swiss V, Casaccia P (2010) Primary brain tumors, neural stem cell, and brain tumor cancer cells: Where is the link? Neuropharmacology:903-910.
Goolsby J, Marty MC, Heletz D, Chiappelli J, Tashko G, Yarnell D, Fishman PS, Dhib-Jalbut S, Bever CT, Jr., Pessac B, Trisler D (2003) Hematopoietic progenitors express neural genes. Proc Natl Acad Sci U S A 100:14926-14931.
Hess DC, Hill WD, Martin-Studdard A, Carroll J (2002) Bone marrow as a source of endothelial cells and NeuN-expressing cells after stroke. Stroke:1362-1368.
Hodgkin AL, Huxley AF (1952) A quantitative description of membrane current and its application to conduction and excitation in nerve. J Physiol 117:500-544.
Jacobs BL, van Praag H, Gage FH (2000) Adult brain neurogenesis and psychiatry: a novel theory of depression. Molecular psychiatry 5:262-269.
Kempermann G (2000) Adult neurogenesis: stem cells and neuronal development in the adult brain. New York: Oxford University Press.
Kempermann G, Kuhn HG, Gage FH (1997) More hippocampal neurons in adult mice living in an enriched environment. Nature 386:493-495.
Kim YF, Sandeman DC, Benton JL, Beltz BS (2014) Birth, survival and differentiation of neurons in an adult crustacean brain. Developmental neurobiology 74:602-615.
Kohyama J, Abe H, Shimazaki T, Koizumi A (2001) Brain from bone: efficient "meta-differentiateion" of marrow stroma-derived mature osteoblasts to neurons with Noggin or a demthylating agent. Differentiation:235-244.
Kokoeva MV, Yin H, Flier JS (2007) Evidence for constitutive neural cell proliferation in the adult murine hypothalamus. The Journal of comparative neurology 505:209-220.
Kokovay E, Shen Q, Temple S (2008) The incredible elastic brain: how neural stem cells expand our minds. Neuron:420-429.
Kopen GC, Prockop DJ, Phinney DG (1999) Marrow stromal cells migrate throughout forebrain and cerebellum, and they differentiate into astrocytes after injection into neonatal mouse brains. Proceedings of the National Academy of Sciences 96:10711-10716.
Liu H, Soderhall I (2006) Histone H2A as a trasfection agent in crayfish hematopoietic tissue cells. Developmental and Comparative Immunology 31:340-346.
Liu J, Solway K, Messing RO, Sharp FR (1998) Increased neurogenesis in the dentate gyrus after transient global ischemia in gerbils. J Neurosci 18:7768-7778.

Magavi SS, Leavitt BR, Macklis JD (2000) Induction of neurogenesis in the neocortex of adult mice. Nature 405:951-955.
Makar TK, Wilt S, Dong Z, Fishman P (2002) IFN-beta gene transfer into the central nervous system using bone marrow cells as a delivery system. Journal of Interferon Cytokine Research:783-791.
Mezey E, Chandross KJ (2000) Bone marrow: a possible alternative source of cells in the adult nervous system. Eur J Pharmacol 405:297-302.
NIH (2015) What are the unique properties of al stem cells? In: Stem cell Information. Bethesda, MD: National Institutes of Health, U.S. departent of Health and Human Services.
Nilsson M, Perfilieva E, Johansson U, Orwar O, Eriksson PS (1999) Enriched environment increases neurogenesis in the adult rat dentate gyrus and improves spatial memory. Journal of neurobiology 39:569-578.
Noonin C, Lin XH, Jiravanichpaisal P, Soderhall K, Soderhall I (2012) Invertebrate Hematopoiesis: An Anterior Proliferation Center As a Link Between the Hematopoietic Tissue and the Brain. Stem Cells and Development 21:3173-3186.
Novus-Biologicals (2015) Antibody Protocol and How to Book, SDS Page & Western Blotting. In: Novus Biologicals, a Biotechne Brand.
Parent JM, Yu TW, Leibowitz RT, Geschwind DH, Soloviter RS, Lowenstein DH (1997) Dentate granule neurogenesis is increased by seizures and contributes to aberrant network reorganization in the adult hippocampus. Journal of Neuroscience 17:3727-3738.
Pun RYK, Rolle IJ, LaSarge CL, Hosford BE, Rosen JM, Uhl JD, Schmeltzer SN, Faulkner C, Bronson SL, Murphy BL, Richards DA, Holland KD, Danzer SC (2012) Excessive Activation of mTOR in Postnatally Generated Granule Cells Is Sufficient to Cause Epilepsy. Neuron 75:1022-1034.
Robinson CD, Lourido S, Whelan SP, Dudycha JL, Lynch M, Isern S (2006) Viral transgenesis of embryonic cell cultures from the freshwater microcrustacean Daphnia. J Exp Zool A Comp Exp Biol 305:62-67.
Rousselot P, Lois C, Alvarezbuylla A (1995) Embryonic (Psa) N-Cam Reveals Chains of Migrating Neuroblasts between the Lateral Ventricle and the Olfactory-Bulb of Adult Mice. Journal of Comparative Neurology 351:51-61.
Ruster B, Gottig S, Ludwig RJ, Bistrian R, Muller S, Seifried E, Gille J, Henschler R (2006) Mesenchymal stem cells display coordinated rolling and adhesion behavior on endothelial cells. Blood 108:3938-3944.
Sanchez-Ramos J, Cardozo-Pelaez F, Song S (1998) Differentiation of neuron-like cells from bone marrow stromal cells. Movement Disorders 13:122.
Sanchez-Ramos J, Song S, Cardozo-Pelaez F, Hazzi C (2000) Adult bone marrow stromal cells differentiate into neural cells in vitro. Experimental Neurology:247-256.
Sandeman D, Sandeman R, Derby C, Schmidt M (1992) Morphology of the Brain of Crayfish, Crabs, and Spiny Lobsters - a Common Nomenclature for Homologous Structures. Biological Bulletin 183:304-326.
Sandeman DC, Benton JL, Beltz BS (2009) An identified serotonergic neuron regulates adult neurogenesis in the crustacean brain. Developmental neurobiology 69:530-545.

Sandeman R, Sandeman D (2000) "Impoverished" and "enriched" living conditions influence the proliferation and survival of neurons in crayfish brain. Journal of neurobiology 45:215-226.
Schmidt M (2007) The olfactory pathway of decapod crustaceans--an invertebrate model for life-long neurogenesis. Chem Senses 32:365-384.
Schmidt M, Demuth S (1998) Neurogenesis in the central olfactory pathway of adult decapod crustaceans. Annals of the New York Academy of Sciences 855:277-280.
Schmidt-Hieber C, Jonas P, Bischofberger J (2004) Enhanced synaptic plasticity in newly generated granule cells of the adult hippocampus. Nature 429:184-187.
Sigma-Aldrich MISSION® pLKO.1-puro-CMV-TurboGFP™ Positive Control Transduction Particles, General Description. In.
Sirav B, Seyhan N (2011) Effects of radiofrequency radiation exposure on blood-brain barrier permeability in male and female rats. Electromagn Biol Med 30:253-260.
Steiner B, Klempin F, Wang L, Kott M, Kettenmann H, Kempermann G (2006) Type-2 cells as link between glial and neuronal lineage in adult hippocampal neurogenesis. Glia 54:805-814.
Steingen C, Brenig F, Baumgartner L, Schmidt J, Schmidt A, Bloch W (2008) Characterization of key mechanisms in transmigration and invasion of mesenchymal stem cells. J Mol Cell Cardiol 44:1072-1084.
Suh H, Consiglio A, Ray J, Sawai T, D'Amour KA, Gage FH (2007) In vivo fate analysis reveals the multipotent and self-renewal capacities of Sox2+ neural stem cells in the adult hippocampus. Cell Stem Cell 1:515-528.
Sullivan JM, Beltz BS (2005) Newborn cells in the adult crayfish brain differentiate into distinct neuronal types. Journal of neurobiology 65:157-170.
Sullivan JM, Benton JL, Sandeman DC, Beltz BS (2007) Adult neurogenesis: a common strategy across diverse species. The Journal of comparative neurology 500:574-584.
Uchida N, Buck D, He D, Reitsma M, Masek M, Phan T, Tsukamoto A, Gage G, Weissman I (2000) Direct isolation of human central nervours system stem cells. Proceedings of the National Academy of Sciences:14720-14725.
van Praag H, Christie BR, Sejnowski TJ, Gage FH (1999) Running enhances neurogenesis, learning, and long-term potentiation in mice. Proc Natl Acad Sci U S A 96:13427-13431.
van Praag H, Schinder AF, Christie BR, Toni N, Palmer TD, Gage FH (2002) Functional neurogenesis in the adult hippocampus. Nature 415:1030-1034.
van Vulpen M, Kal HB, Taphoorn MJ, El-Sharouni SY (2002) Changes in blood-brain barrier permeability induced by radiotherapy: implications for timing of chemotherapy? (Review). Oncol Rep 9:683-688.
Woodbury D, Schwarz EJ, Prockop DJ, Black IB (2000) Adult rate and human bone marrow stromal cells differentiate into neurons. Journal of Neuroscience Research:364-370.
Zhang Y, Allodi S, Sandeman DC, Beltz BS (2009) Adult neurogenesis in the crayfish brain: proliferation, migration, and possible origin of precursor cells. Developmental neurobiology 69:415-436.
Zhao C, Deng W, Gage FH (2008) Mechanisms and functional implications of adult neurogenesis. Cell 132:645-660.

Zufferey R, Donello JE, Trono D, Hope TJ (1999) Woodchuck hepatitis virus posttranscriptional regulatory element enhances expression of transgenes delivered by retroviral vectors. J Virol 73:2886-2892.